

# RF Free Ultrasonic Positioning\*

Michael R McCarthy Henk L Muller

Department of Computer Science, University of Bristol, U.K.

<http://www.cs.bris.ac.uk/home/mccarthy/>

## Abstract

*All wearable centric location sensing technologies must address the issue of clock synchronisation between signal transmitting systems and signal receiving systems. GPS receivers, for example, compensate for synchronisation errors by incorporating a model of the receiver clock offset in the navigation solution. Drift between satellite clocks is also monitored to keep signal data in synch with GPS time. Most ultrasonic positioning systems solve the synchronisation problem by using a second medium for communication between transmitter and receiver devices. The transmitters in these systems emit RF signals (pings) to indicate the transmission of subsequent ultrasound signals (chirps). By subtracting the arrival time of the ping from that of the chirps, the receiver is able to compute the distance to each transmitter.*

*In this paper, we describe an ultrasonic positioning system that does not use RF signals to achieve synchronisation. Instead, it exploits a periodic chirp transmission pattern to model the receiver's position using chirp reception times exclusively. Not only does the system improve on the accuracy of previous technologies but it also eliminates bulky RF circuitry – a definite advantage for wearable applications where component size and weight are critical for usability.*

## 1 Introduction

Our goal is to develop a passive, wearable centric positioning system. Building on the University of Bristol's previous solution [11], we maintain that cost, weight and size are of critical importance for use within a wearable framework. Our new approach improves on its predecessor in two important ways. First, by eliminating the need for RF we are able to reduce the size and weight of the ultrasonic receiver considerably. Large RF chips and cumbersome antennae, that quite often consume more than fifty percent of

the receiver configuration, are no longer required. The receiver is reduced to a single ultrasonic microphone and its accompanying amplification circuitry.

The second improvement achieved with an RF free solution is the elimination of clock synchronisation errors. These errors are particularly evident in systems that use pings to indicate the start of a chirp transmission sequence. For example, rather than use a ping to indicate the transmission of a single chirp [10, 15], Bristol's system uses a ping to indicate the start of a transmission cycle, within which four or more chirps may be transmitted. There is an agreement between the transmitter and receiver as to the length of delay between transmission of the ping and subsequent chirps. We have been able to demonstrate that the actual delay used by the transmitter and the delay experienced by the receiver are not consistent, especially for chirps late in the sequence. This observation is a direct result of the different frequencies of the transmitter and receiver clocks, producing errors in the calculation of transmitter-receiver distances. By eliminating the RF synchronisation mechanism and the associated assumption of equal clock frequencies we are able to eliminate these errors.

The RF free transmitter transmits chirps at regular intervals and in a known pattern. This, along with knowledge of transmitter locations, is all that a receiver needs to calculate its position. GPS receivers face a similar challenge, where the position of the satellites is also known. The major difference between the two systems, however, is that GPS receivers have access to signal transmission times encoded in the signal [5]. They need only compensate for receiver synchronisation issues (offset from GPS time) to determine distance to the satellites. Our receivers, on the other hand, must extract transmission times by exploiting the periodic nature of the transmitter system.

## 2 Problem

The transmitter used in the RF free system is constructed in a similar fashion to the system designed at the University of Bristol [11]. Four transmitters are placed in a square on the ceiling of a room and are activated in a cyclic pattern as

---

\*Funding for this work is received from the U.K. Engineering and Physical Sciences Research Council, Grant No. GR/N15986/01.



Combining this result with Equation 1, we are able to calculate  $U_0$ :

$$U_0 = R_k - t_k - kP \quad (5)$$

In this equation,  $k$  refers to the first chirp in any four chirp sequence (labelled  $t_0$  in Equation 3). Because we incorporate four chirps at every step of the KF,  $k$  is incremented by four after each step.

The two variables  $P$  and  $U_0$  completely describe the time-varying transmitter process. The system tracks them as the states of the KF. The state equations are as follows:

$$\begin{aligned} P &= P_{\text{previous}} \\ U_0 &= U_{0\text{previous}} \end{aligned} \quad (6)$$

The KF measures  $U_0$  indirectly by pre-processing the chirp reception times using Equations 3 and 5. It also measures  $P$  indirectly by subtracting reception times of subsequent chirps originating from the same transmitter.

$$\begin{aligned} 4P &= U_k - U_{k-4} \\ &= (U_k + t_k) - (U_{k-4} + t_{k-4}) \\ &= R_k - R_{k-4} \end{aligned} \quad (7)$$

As before, this equation assumes that the receiver does not move between successive measurements, ie.  $t_k = t_{k-4}$ .

### 3.2 Results

The KF was tested with two ten-minute data sets: one with a stationary receiver and one with the receiver moving around the room. Figure 2 shows plots of measured values for  $P$  and  $U_0$  versus their filtered equivalents for the stationary data set. It illustrates how the KF is able to converge on values that are much more accurate than the raw measurements. The top figure shows that the measured values for  $P$  are accurate to within  $\pm 2 \mu\text{s}$  while filtered  $P$  in the middle diagram is accurate to within  $\pm 20 \text{ ns}$  after 40 seconds. The lowest plot shows the measured value for  $U_0$  – accurate to within  $\pm 200 \mu\text{s}$  – with its filtered counter-part performing significantly better.

During the second trial, the receiver was moved around the room at random. Figure 3 illustrates how the values of  $P$  and  $U_0$  converge as they did in the first trial but are disturbed by the movement of the receiver. The spikes in the plots result from the assumption in the measurement equations (2 and 7) that the receiver is motionless. When the receiver moves, the equations become inconsistent and the filter attempts to compensate by adjusting  $P$  and  $U_0$ . In the next section we demonstrate a solution that eliminates this undesirable behaviour.

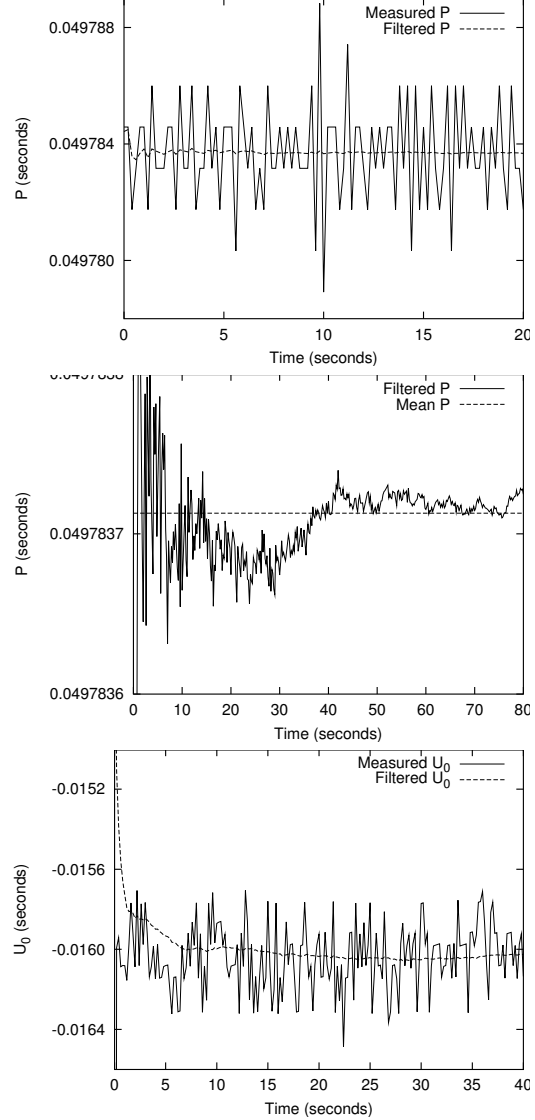
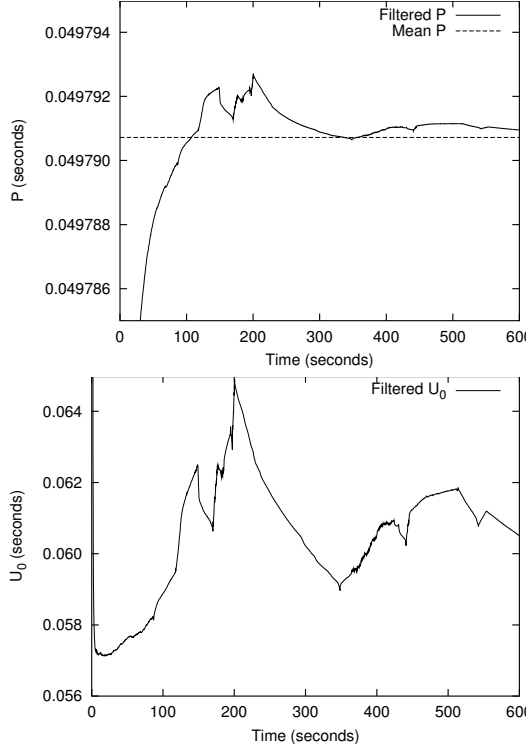


Figure 2. Transmitter Model: Stationary Receiver

## 4 Position Model

To improve on the results of the previous section, we incorporate some of the *hidden dynamics* neglected in the previous design. In particular, the relationship between the receiver position and the transmitter operation are unknown to the filter in the Transmitter Model, where the dynamics are concealed in the measurement pre-processing equations. By defining the time-of-flight of chirp  $k$  (originating from transmitter  $i$ ) as:

$$t_k = \sqrt{(x - X_i)^2 + (y - Y_i)^2 + (z - Z_i)^2} \quad (8)$$



**Figure 3. Transmitter Model: Moving Receiver**

and manipulating Equation 5, we are able to formulate an equation that expresses chirp reception times in terms of five unknown variables ( $P$ ,  $U_0$ ,  $x$ ,  $y$ ,  $z$ ):

$$R_k = \sqrt{(x - X_i)^2 + (y - Y_i)^2 + (z - Z_i)^2} + U_0 + kP \quad (9)$$

Again, in this equation,  $U_0$  refers to the transmission time of the first chirp since the *start* of the system. For simplicity, we omit the speed of sound by redefining position in terms of time-distances. In the case of the x-axis, for example, we observe  $x = x_{\text{actual}}/v$  where  $v$  is the speed of sound. Transmitter positions are represented in this form as well.

#### 4.1 Filter Design

The state vector contains the five unknown random variables.

$$\mathbf{x} = [P \ U_0 \ x \ y \ z]^T \quad (10)$$

For this iteration of the filter design, we assume that movements of the receiver are a result of noise in the process

dynamics. In other words, we hide receiver velocity from the filter. As a result, the state transition matrix,  $\mathbf{A}$ , is the identity matrix, defining the state – which includes position – as constant over time.

The convenient consequence of including the process dynamics in the KF is that measurement pre-processing is no longer required. The chirp reception times are passed directly to the filter as the measurements. We use Equation 9 to define the relationship between chirp reception times and the state, nominating it as the KF measurement sensitivity equation. However, in order to use this non-linear equation in our model, we must linearise it by applying the Extended Kalman Filter (EKF) method. In an EKF, the measurement sensitivity matrix,  $\mathbf{H}_k$  (a Jacobian matrix), is derived from the partial derivatives of the measurement sensitivity equation, evaluated at the current state. In our design,  $\mathbf{H}_k$  is computed from the partial derivatives of Equation 9 at every time-step.

Our problem is also specially suited for a technique of measurement integration known as *single constraint at a time* (SCAAT) [17]. This method allows reception times to be incorporated into the filter as they are observed (instead of waiting for a complete chirp sequence), improving the response time of the system as well as reducing computational overhead (see [17]). Employing SCAAT means that the step counter of the filter is equal to  $k$ , which counts chirps originating from transmitters identified by  $k \bmod n$ , where  $n$  is the number of transmitters.

It is also important to note that this solution does not depend on the orientation of the transmitters. Unlike the Transmitter Model, which relies on Equation 2, the Position Model only requires that the location of the transmitters be known. In the next section we describe results from trials using a six-transmitter system where the square topology shown in Figure 1 is supplemented with two transmitters located outside of the plane.

#### 4.2 Results

Again, the EKF was tested with two data sets, the stationary test with two minutes of data and the moving test with approximately three minutes of data.

The first test is the stationary test, where the receiver was left at position (0.21 m, -0.40 m, -1.53 m). The top two graphs of Figure 4 illustrate how the filter closes in on values for  $P$  and  $U_0$  during this test. Figure 5 shows the position of the receiver in terms of its co-ordinates in the room ( $x$ ,  $y$ ,  $z$ ). With regards to accuracy, the calculated standard deviations are 6 mm, 5 mm, and 40 mm in the  $x$ ,  $y$ , and  $z$  directions, respectively.

The second test was done with a moving receiver. Throughout the test, the receiver height ( $z$ ) was held constant at -1.53m while  $x$  and  $y$  were varied within a 2 m

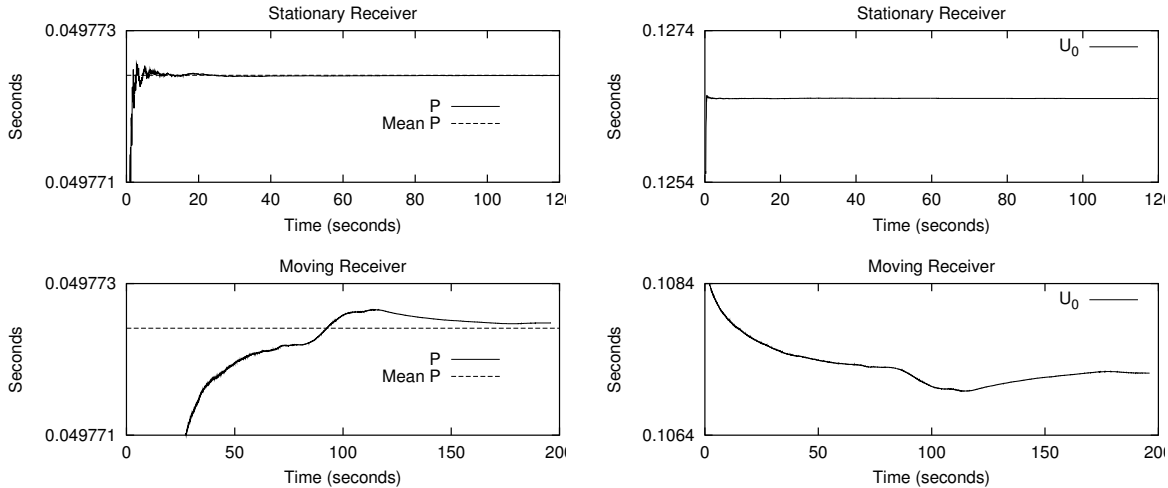


**Figure 4. Convergence of  $P$ ,  $U_0$**

square area. The two graphs at the bottom of Figure 4 show the convergence of  $P$  and  $U_0$  during this test. As expected, the results are better than those achieved with just the Transmitter Model (Figure 3). It is also apparent that the Position Model converges to more accurate values for  $P$  and  $U_0$  in the stationary test than it does for the moving test. This is a predicted observation where, in the case of the moving test, the unmodelled receiver motion results in an increase in the system error. The increase in error affects the stability of all of the state variables, including  $P$  and  $U_0$ . We expect that improving the dynamic model – by including velocity – will enhance the filter’s performance in this respect.

The  $x$ ,  $y$ , and  $z$  co-ordinates for the moving receiver path are displayed in Figure 6. The standard deviation for  $z$  in this test is 10 cm. To calculate the error in the  $x$  and  $y$  directions, we use the Projected Standard Deviation method [12] over the variances displayed in Figure 7 (a close-up of the region highlighted in Figure 6 where our system performs the worst). The Projected Standard Deviation over this region of maximum variance is approximately 5 cm.

The deflections or variances in the path are caused by the SCAAT method, where the state is updated one measurement at a time. There are certain locations on the path where these variances are larger than others, for example, the region illustrated in Figure 7. We have determined that, at these locations, the chirps arrive at the receiver from shallow angles, resulting in degraded chirps and skewed measurements of reception time. A better transmitter topology and a model of measurement degradation based on angle and distance from the transmitters should reduce the size of these variances. Again, we also expect that improving the dynamic model will help with this as well.

The error along the  $z$  axis is noticeably larger than that

CPU	% of Real-time
Athlon (1.6G Hz)	0.05
StrongARM (200 MHz)	4.08

**Table 1. Percentage of Real-time Execution**

of the  $x$  and  $y$  axes for both the stationary and moving tests. This is a result of a higher dilution of precision (DOP) in the  $z$  direction, a characteristic inherent to the placement of the transmitters. For the configuration used in this section, the space between the transmitters is much larger along the  $x$  and  $y$  axes and, therefore, provides better accuracy in these directions [5]. The result gives motivation for avoiding transmitter arrangements that are planar, such as that discussed in Section 3. In a planar configuration the DOP in the  $z$  direction is extremely high.

For all of the tests, the filter is able to compute the receiver’s location in real-time. Table 1 shows the execution time of the moving test as a percentage of real-time execution. The test was performed on two different machines: a PC with a 1.6 GHz Athlon processor and a wearable computer with a 200 MHz StrongARM processor. The results show that both processors are able to comfortably handle the computational load. Additionally, the performance of the algorithm can be improved further by optimising the matrix operations executed during each step of the Kalman filter.

Execution time, and hence computational complexity, is inversely related to the period of chirp transmission,  $P$ . Decreasing  $P$  increases the number of step operations that the Kalman filter performs for a fixed period of time. However,  $P$  has a physical lower bound beyond which collisions

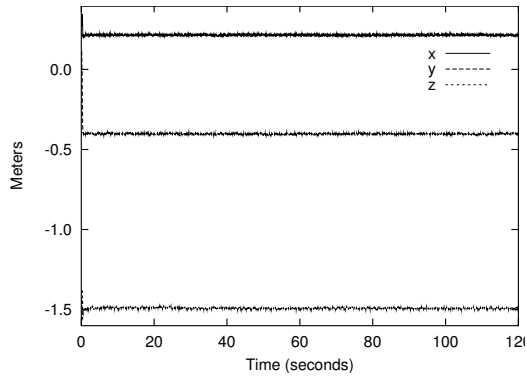


**Figure 5. Stationary Receiver Path**

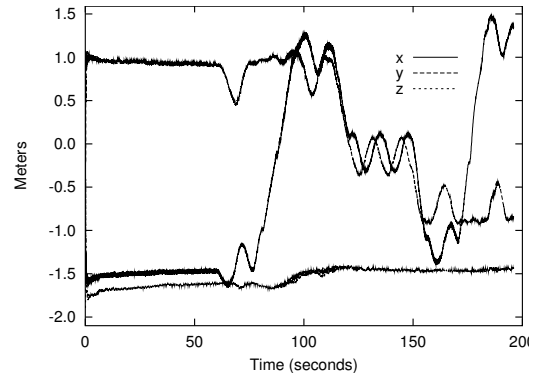
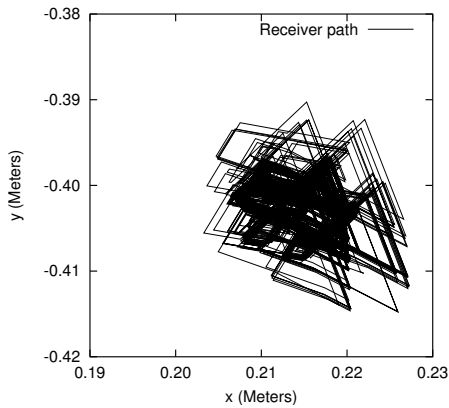
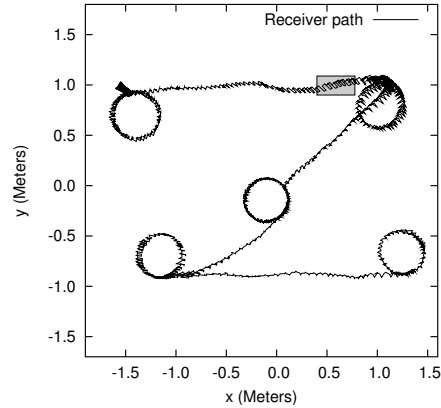


**Figure 6. Moving Receiver Path**



between sequential transmissions becomes highly probable. The bound imposed by processor resources is much lower than this physical bound and is thus ignored. The number of transmitters used in the system does not affect computational complexity. For example, adding transmitters to the system only decreases the frequency at which each transmitter is activated – the time between the processing of each chirp ( $P$ ) is not affected. For six transmitters the storage requirements is around 180 bytes. The code is 8.7 kilobytes binary. We hope that it will fit on the dsPIC<sup>®</sup> devices that Microchip are expected to release at the end of 2003.

## 5 Conclusion

We have demonstrated that it is not necessary to use RF in an ultrasonic positioning system for wearable computers. Our system shows that it is possible to model the position of a wearable receiver using chirp reception times only. This is achieved by exploiting the periodic transmission interval in the RF free transmitter. The system is able to extract  $x$ ,  $y$ , and  $z$  co-ordinates with a fairly high degree of accuracy ( $\sim 10$  cm for the moving tests).

Eliminating the RF components on the receiver circuit

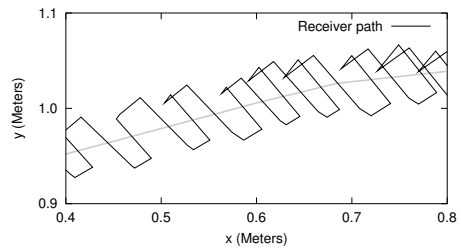


**Figure 7. Moving Receiver Path Close-up**

gives advantages in terms of wearability, price and power consumption. As a sensor, the receiver is smaller and easier to embed in a wearable framework. Fewer components means that the cost of the overall system is reduced as well. In terms of power consumption, an RF free receiver offers increased battery longevity. Although the computational load on the receiver is greater with the introduction of a Kalman filter, this is more than accounted for by the reduction in the number of powered components in the circuit. We hope to run the system on a low power DSP such as the Microchip dsPIC<sup>®</sup>.

There are also privacy advantages to our system. Unlike

other ultrasonic solutions available today, our system is not a *tracker*. The infrastructure is unintelligent. It provides only simple reference points that the receiver uses to compute location; very much in the same way that GPS works. This information is proprietary to the wearable system, an important feature for applications where privacy is a concern.

## 6 Future Work

All narrowband ultrasonic positioning systems are faced with the problem of in-band noise, occlusions and chirp collisions. Although excellent work has been done to alleviate these problems using broadband ultrasound [6], we believe that narrowband systems can still be improved. In future versions of the system design we hope to use our model to handle missing or anomalous measurements from noise or reflections. By observing measurement residuals, for example, the Kalman filter can be used to determine measurement quality. We hope that, at the very least, residual analysis will allow us to identify outliers so as to prevent them from corrupting the system.

Other improvements to the system will involve developing the dynamic position model further. Augmenting the state with higher order dynamics, such as velocity, should improve the system's response to receiver movement. Introducing a model for measurement error with respect to transmitter angle and distance should also improve performance and, hopefully, eliminate unwanted deflections in the receiver path.

## Acknowledgements

Many thanks to Cliff Randell for conceiving the first ultrasonic system at the University of Bristol.

## References

- [1] R. G. Brown and P. Y. Hwang. *Introduction to Random Signals and Applied Kalman Filtering*. Wiley, Inc, third edition, 1997.
- [2] J. V. Candy. *Signal Processing: The Model Based Approach*. McGraw-Hill, Inc., 1986.
- [3] A. Gleb. *Applied Optimal Estimation*. MIT Press, 1974.
- [4] M. S. Grewal and A. P. Andrews. *Kalman Filtering: Theory and Practice*. Prentice-Hall, Inc., 1993.
- [5] M. S. Grewal, L. R. Weill, and A. P. Andrews. *Global Positioning Systems, Inertial Navigation, and Integration*. Wiley, Inc., 2001.
- [6] M. Hazas and A. Ward. A novel broadband ultrasonic location system. In G. Borriello and L. E. Holmquist, editors, *UbiComp 2002: Ubiquitous Computing*, pages 264–280, Göteborg, Sweden, September 2002. Springer-Verlag.
- [7] Intersense Inc. Website. <http://www.isense.com/>, 2003.
- [8] R. E. Kalman. A new approach to linear filtering and prediction problems. *Journal of Basic Engineering (ASME)*, 82(D):35–45, March 1960.
- [9] P. S. Maybeck. *Stochastic models, estimation, and control*, volume 141 of *Mathematics in Science and Engineering*. 1979.
- [10] N. B. Priyantha, A. Chakraborty, and H. Balakrishnan. The cricket location-support system. In *Mobile Computing and Networking*, pages 32–43, 2000.
- [11] C. Randell and H. Muller. Low cost indoor positioning system. In G. D. Abowd, editor, *UbiComp 2001: Ubiquitous Computing*, pages 42–48. Springer-Verlag, September 2001.
- [12] C. Randell and H. L. Muller. Exploring the dynamic measurement of position. In M. Billinghurst, editor, *Sixth International Symposium on Wearable Computers*, pages 117–124. IEEE Computer Society, October 2002.
- [13] H. W. Sorenson. Least-squares estimation: from Gauss to Kalman. *IEEE Spectrum*, 7:63–68, July 1970.
- [14] A. Ward. *Sensor-driven Computing*. PhD thesis, University of Cambridge, August 1998.
- [15] A. Ward, A. Jones, and A. Hopper. A new location technique for the active office. *IEEE Personnel Communications*, 4(5):42–47, October 1997.
- [16] G. Welch and G. Bishop. An introduction to the Kalman filter. Technical Report TR95-041, Department of Computer Science, University of North Carolina - Chapel Hill, November 1995.
- [17] G. Welch and G. Bishop. SCAAT: Incremental tracking with incomplete information. *Computer Graphics*, 31(Annual Conference Series):333–344, 1997.
- [18] G. Welch, G. Bishop, L. Vicci, S. Brumback, K. Keller, and D. Colucci. Highperformance wide-area optical tracking: The HiBall tracking system. *Teleoperators and Virtual Environments*, 10(1), 2001.